eNeuro

Research Article: New Research | Disorders of the Nervous System

Alterations in Cytosolic and Mitochondrial [U-^{13}C]-Glucose Metabolism in a Chronic Epilepsy Mouse Model

Decreased TCA cycling in epilepsy

Tanya S. McDonald[1], Catalina Carrasco-Pozo[1,2], Mark P. Hodson[2,3] and Karin Borges[1]

[1]*Department of Pharmacology, School of Biomedical Sciences, the University of Queensland, QLD 4072, Australia St. Lucia*

[2]*Department of Nutrition, Faculty of Medicine, University of Chile, Santiago 8380453 PO Box*

[3]*Metabolomics Australia, Australian Institute for Bioengineering and Nanotechnology, the University of Queensland, QLD 4072, Australia St. Lucia*

[4]*School of Pharmacy, the University of Queensland, QLD 4072, Australia St Lucia*

DOI: 10.1523/ENEURO.0341-16.2017

Received: 14 November 2016

Revised: 10 January 2017

Accepted: 16 January 2017

Published: 10 February 2017

Author contributions: T.S.M. and K.B. designed research; T.S.M., C.C.-P., and M.P.H. performed research; T.S.M., C.C.-P., and M.P.H. analyzed data; T.S.M., C.C.-P., M.P.H., and K.B. wrote the paper.

Authors report no conflict of interest

Department of Health | National Health and Medical Research Council (NHMRC) 1044007; Fondecyt Initiation into Research Grant 11130232.

Correspondence should be addressed to Tanya S. McDonald, Department of Pharmacology, School of Biomedical Sciences, Skerman Building 65, St Lucia, QLD 4072, Australia, E-mail: tanya.mcdonald@uqconnect.edu.Au

Cite as: eNeuro 2017; 10.1523/ENEURO.0341-16.2017

Alterations in cytosolic and mitochondrial [U-^{13}C]-glucose metabolism in a chronic epilepsy mouse model

Abbreviated title: Decreased TCA cycling in epilepsy

Tanya S. McDonald[1], Catalina Carrasco-Pozo[1,2], Mark P. Hodson[2,3], Karin Borges [1]

[1] Department of Pharmacology, School of Biomedical Sciences, The University of Queensland, St. Lucia QLD 4072, Australia

[2]Department of Nutrition, Faculty of Medicine, University of Chile, PO Box 8380453, Santiago

[3] Metabolomics Australia, Australian Institute for Bioengineering and Nanotechnology, The University of Queensland, St. Lucia QLD 4072, Australia

[4] School of Pharmacy, The University of Queensland, St Lucia, QLD 4072, Australia

Corresponding author:

Tanya McDonald BBiomedSc (Hons)

Department of Pharmacology

School of Biomedical Sciences

Skerman Building 65

St Lucia, QLD 4072, Australia

(+617) 3365 3659

E-mail: tanya.mcdonald@uqconnect.edu.au

Number of Figures: 4

Number of Tables: 2

Number of words:

Abstract: 250

Introduction: 458

Discussion: 1683

Conflict of interest: The authors declare no conflict of interest.

Acknowledgements

We are grateful for funding from NHMRC (project grant 1044007 to KB), Fondecyt Initiation into Research (Grant 11130232 to CC) and APA scholarship (TM).

Abstract

Temporal lobe epilepsy is a common form of adult epilepsy and shows high resistance to treatment. Increasing evidence has suggested that metabolic dysfunction contributes to the development of seizures, with previous studies indicating impairments in brain glucose metabolism. Here we aim to elucidate which pathways involved in glucose metabolism are impaired by tracing the hippocampal metabolism of injected [U-^{13}C]-glucose (i.p.) during the chronic stage of the pilocarpine-status epilepticus mouse model of epilepsy. The enrichment of ^{13}C in the intermediates of glycolysis and the TCA cycle were quantified in hippocampal extracts using liquid chromatography tandem mass spectroscopy, along with the measurement of the activities of enzymes in each pathway. We show that there is reduced incorporation of ^{13}C in the intermediates of glycolysis, with the percent enrichment of all downstream intermediates highly correlated to those of glucose 6-phosphate. Furthermore, the activities of all enzymes in this pathway including hexokinase and phosphofructokinase were unaltered, suggesting that glucose uptake is reduced in this model without further impairments in glycolysis itself. The key finding was a 33% and 55% loss in the activities of pyruvate dehydrogenase and 2-oxoglutarate dehydrogenase, respectively, along with reduced ^{13}C enrichment in TCA cycle intermediates. This lower ^{13}C enrichment is best explained in part due to the reduced enrichment in glycolytic intermediates, while the reduction of key TCA cycle enzyme activity indicates that the TCA cycling is also impaired in the hippocampal formation. Together this study suggests that multi-target approaches may be necessary to restore metabolism in the epileptic brain.

Key words: epilepsy, glucose metabolism, glycolysis, mitochondria, seizure, tricarboxylic acid cycle

Significance statement

The specific metabolic impairments that occur in the epileptic brain and can play a role in the development of seizures are mostly unknown. Glucose uptake has been shown to be reduced in epileptic brain areas in patients and models. By following ^{13}C-glucose metabolism, we show that during the chronic epileptic stage in a murine model, there are further impairments to oxidative glucose metabolism along with reduced maximal activities of pyruvate dehydrogenase and 2-oxoglutarate dehydrogenase, key enzymes of the TCA cycle in the hippocampus. Together with diminished glucose uptake, this will decrease the ability to produce ATP in epileptogenic areas, which may contribute to seizure development. This research identified new targets for new therapies to inhibit seizures in the "epileptic" brain.

Introduction

Temporal lobe epilepsy (TLE) is one of the most common forms of epilepsy in adults with approximately one-third of patients being multi-drug resistant. Many of the pathophysiological characteristics and the chronic spontaneous seizures of TLE are reflected in rodents after pilocarpine-induced status epilepticus (SE) (Borges et al., 2003b). Epileptic disorders are often associated with genetic mutations (Mulley et al., 2005; Escayg and Goldin, 2010), inflammation (Vezzani et al., 2011), and an imbalance between excitatory and inhibitory neurotransmission (Avoli et al., 2016). In addition there is growing evidence that dysfunction in metabolic pathways within brain tissue such as glycolysis, the TCA cycle and electron transport chain contribute to the initiation and progression of seizures (Alvestad et al., 2011; Tan et al., 2015).

In patients with TLE, numerous positron emission tomography (PET) studies using ^{18}F-labelled fluorodeoxyglucose (^{18}FDG) have shown that during a seizure event glucose uptake is increased, whereas less glucose is taken up interictally in the epileptogenic zone (Kuhl et al., 1980; Chugani and Chugani, 1999; Vielhaber et al., 2003). In the chronic rat lithium-pilocarpine model of epilepsy, local cerebral glucose utilization rates ($LCMR_{glcs}$) were reduced in several brain regions in between seizures, including the hippocampal CA1 and CA3 areas as determined by the use of ^{14}C-2-deoxyglucose (^{14}C-2DG) (Dube et al., 2001). The limitations of these studies are that after metabolism via hexokinase the 6-phosphates of ^{18}FDG and ^{14}C-2DG are not substrates for subsequent glycolytic reactions. Thus, these studies cannot provide any indication relating to further changes in glucose metabolism. The metabolism of glucose has previously been studied in both the pilocarpine- and lithium pilocarpine-induced SE rodent models. Elevated hippocampal glucose concentrations were observed in the chronic stage of the lithium pilocarpine rat model, however no change was found in the concentrations of [1-^{13}C]-glucose (Melo et al., 2005). Despite this lack of change in [1-^{13}C]-glucose amounts, the concentrations of glutamate and GABA, resulting from [1-^{13}C]-glucose metabolism were lower in the SE mice during the chronic phase. Similarly, in the mouse pilocarpine model we found a lower percent enrichment of ^{13}C derived from [1,2-^{13}C]-glucose metabolism in citrate, malate and the amino acids GABA and aspartate without a change in glucose concentrations or the percent enrichment of [1,2-^{13}C]-glucose (Smeland et al., 2013). Together these results suggest that glucose metabolism is perturbed in chronic epileptic rodent models, which may be a result of recurrent seizures but also may contribute to seizure development.

Although previous studies have indicated a disturbance in glucose metabolism in the chronic epileptic brain, it is unclear where the perturbation in glucose metabolism occurs. Here, we

performed a comprehensive study of glucose metabolism, using the mouse pilocarpine SE model to determine the changes that occur in hippocampal glucose metabolism during the chronic "epileptic" stage with the use of [U-^{13}C]-glucose.

Materials and Methods

Animals

Male CD1 mice (Australian Research Council, WA, Australia) were individually caged under a 12-hour light-dark cycle with standard diet as used in previous studies (SF11-027, Specialty feeds, Western Australia, Australia) (Hadera et al., 2013; McDonald et al., 2013) and water given *ad libitum*. The animals were adapted to conditions for at least 1 week, and were between 7-8 weeks old when used in experiments. All efforts were made to minimise the suffering and number of animals used. All experiments were approved by the University of Queensland's Animal Ethics Committee and followed the guidelines of the Queensland Animal Care and Protection Act 2001. This work was performed according to the ARRIVE guidelines (https://www.nc3rs.org.uk/arrive-guidelines).

Pilocarpine status epilepticus model

As described previously (Smeland et al., 2013), mice were injected with methylscopolamine (2 mg/kg intraperitoneally in 0.9% NaCl; Sigma Aldrich, St Louis, MO, USA) 15 minutes prior to pilocarpine (345 mg/kg subcutaneously in 0.9% saline; Sigma Aldrich). After a 90 minute observation period mice were injected with pentobarbital (22.5 mg/kg intraperitoneally in 0.9% NaCl; Provet, Northgate, QLD, Australia) to stop SE. Mice were defined as developing SE if they were observed to have continuous seizure activity mainly consisting of whole-body clonic seizures. Those that did not display this behaviour were classified as No SE.

[U-^{13}C]-glucose Injections and Tissue Extraction

Three weeks after SE, 10 SE mice and 11 No SE mice were injected with [U-^{13}C]-glucose (0.3 mol/L intraperitoneally, 558 mg/kg; 99% ^{13}C; Cambridge Isotope Laboratories, Wobum, MA, USA). To denature brain enzymes and other proteins immediately, mice were sacrificed by focal microwave fixation to the head at 5 kW for 0.79 to 0.83 seconds (Model MMW-05, Muromachi, Tokyo, Japan) 15 minutes after [U-^{13}C]-glucose injections. Mice were then decapitated and hippocampal formations dissected out and stored at -80°C until extracted. Samples were sonicated in 1 mL of methanol using a Vibra Cell sonicator (Model VCX 750, Sonics and Materials, Newton, CT, USA) with 4 µL of a 1 mM azidothymidine (AZT) solution added as an internal standard. Polar metabolites were extracted from samples using a modified Bligh-Dyer water/methanol/chloroform extraction procedure at a 2/2/3 ratio as previously described (Le Belle et al., 2002). Samples were lyophilized, reconstituted and stored at -80°C until analysed.

Liquid Chromatography Tandem Mass Spectrometry (LC-MS/MS)

Intermediates of [U-^{13}C]-glucose were analysed following the method described in Medina-Torres et al (2015) with modifications and additions to scheduled multiple reaction monitoring (sMRM) transitions to account for variable carbon labelling patterns (Medina-Torres et al., 2015). These sMRM transitions for all the unlabelled metabolites and their associated instrument parameters are detailed in Table 1.

Analysis of incorporation of ^{13}C in glycolytic and TCA cycle intermediates

[U-^{13}C]-glucose can enter both neurons and astrocytes via the glucose transporters GLUT3 and GLUT1 respectively. Once inside the cell [U-^{13}C]-glucose is phosphorylated to [U-^{13}C]-

158 glucose 6-phosphate which can continue through the glycolytic pathway producing glycolytic
159 intermediates that are all uniformly labelled as shown in Figure 1. These glycolytic
160 intermediates can be measured using LC-MS/MS by first isolating the precursor ion (Q1
161 mass, Da) that is uniformly labelled with ^{13}C. The masses isolated are glucose 6-phosphate
162 (G6P), 265; fructose 6-phosphate (F6P), 265; fructose 1,6-phosphate (F16BP), 345;
163 dihydroxyacetone phosphate (DHAP), 172; 2 and 3 phosphoglycerate (2+3PG), 188;
164 phosphoenolpyruvate (PEP), 170; and pyruvate (PYR), 90. Following collision-induced
165 dissociation (Q2) the product ion detected (Q3 mass) for most glycolytic metabolites was
166 dihydrogen phosphate ion (97 Da). For phosphoenolpyruvate the product ion detected was a
167 phosphite ion (79 Da) and pyruvate loses a carboxyl group resulting in a detectable mass of
168 45 Da.
169 [U-^{13}C]-pyruvate resulting from glycolysis can produce [U-^{13}C]-lactate or alternatively enter
170 the TCA cycle via pyruvate dehydrogenase (PDH, EC 1.2.4.1) to [1,2-^{13}C]-acetyl CoA. This
171 entry of ^{13}C labelled acetyl-CoA results in two ^{13}C carbons in all TCA cycle metabolites
172 (Figure 1). Thus, M+2 isomers are isolated as the precursor ions (Q1, Da), for citrate
173 (CIT),193; aconitate (ACO), 175; 2-oxoglutarate (2OG), 147; succinate (SUC), 119; fumarate
174 (FUM), 117; and malate (MAL), 135. In the collision cell all TCA cycle intermediates lose
175 the carboxyl group. As the ^{13}C is within one of the carboxyl groups of all metabolites after
176 the collision, either one or two ^{13}C-carbons remain on the product ion (Q3). Thus molecular
177 weight (Da) of the product ions are 112 (lost a ^{13}C in the collision, M+1) and 113 (both ^{13}C
178 remain, M+2) for citrate; 85 and 86 aconitate; 102 and 103, 2-oxoglutarate; 72 and 73,
179 fumarate; 72 and 73, malate are produced. The sum of both product ions' percent enrichment
180 is representative of the first turn of the TCA cycle.
181 After the first turn, the resultant [1,2-^{13}C]- or [3,4-^{13}C]-oxaloacetate can again condense with
182 [1,2-^{13}C]-acetyl CoA (Figure 1). This results in M+4 citrate, which can be detected similar to

above with the ions 195 (Q1) and then Q3 is either 114 (M+3) or 115 (M+4). Through the conversion of citrate to 2-oxoglutarate a ^{13}C may be lost and thus the precursor ion for 2-oxoglutarate will be M+3 (148 Da, Q1 ion; 103 or 104 Da, Q3 ions). Alternatively, all four ^{13}C carbons will be retained resulting in an M+4 precursor ion with both carboxyl groups containing a labelled carbon, one of which will be lost in the collision cell (149 Da, Q1; 104 Da, Q3). The remaining intermediates succinate, fumarate and malate that can be measured will all contain three labelled carbons, with the possibility of retaining all or losing one ^{13}C after the collision. Therefore, the molecular weight of the precursor ions isolated are 120, succinate; 118, fumarate and 136, malate; with then 75 and 76 Da ions detected in Q3, and 73 and 74 Da for both fumarate and malate.

Enzyme activities

Mice were decapitated under light isoflurane anaesthesia. The brain was removed and hippocampal formations dissected out and stored at -80°C until used. Mitochondria were isolated as previously described (Tan et al., 2016). Aliquots were stored at -80°C and used to determine mitochondrial enzyme activities

The activities of all enzymes were measured with the Spectromax 190 Microplate reader (Molecular Devices, Sunnyvale, CA, USA) via continuous spectrophotometric assays. All enzymes activities were normalized to protein content, measured via a Pierce Bicinchoninic acid (BCA) assay (ThermoFisher Scientific, Scoresby, Victoria, Australia).

Hexokinase (HK, EC 2.7.1.1), phosphoglucose isomerase (PGI, EC 5.3.1.9) and glucose 6-phosphate dehydrogenase (G6PDH, EC 1.1.1.49), phosphofructokinase (PFK, EC 2.7.1.11), pyruvate kinase (PK, EC 2.7.1.40), lactate dehydrogenase (LDH, EC 1.1.1.27) and citrate synthase were measure as previously described (Tan et al., 2016). Pyruvate dehydrogenase (PDH, EC 1.2.4.1) was measured using the MTT-PMS method (Ke et al., 2014).

Several enzyme activities were measured through the oxidation of reduced β-nicotinamide adenine dinucleotide (NADH) including glutamate dehydrogenase (GLDH, EC 1.4.1.2), glutamic pyruvic transaminase (GPT, EC 2.6.1.2) and glutamic oxaloacetic transaminase (GOT, EC 2.6.1.1).The GDH assay was initiated with 10 mM 2-oxoglutarate (2-OG), added to a reaction mix containing 100 mM potassium phosphate (pH7.4), 100 mM ammonium chloride and 0.6 mM β-NADH. GPT was measured in 100 mM triethanolamine buffer (pH 7.4), 0.6 mM β-NADH, 50 mM 2-OG and 10 U/mL LDH (L2500, Sigma Aldrich). GOT activity was measured in 80 mM Tris HCl (pH 7.8), 0.6 mM β-NADH, 15 mM 2-OG and 5 U/mL malic dehydrogenase (M1567, Sigma Aldrich) and initiated with the addition of 10 mM aspartate.

The activity of 2-oxoglutarate dehydrogenase (2-OGDH) was measured via the reduction of nicotinamide adenine dinucleotide (β-NAD^+) in 75 mM Tris HCl (pH 8), 1 mM ethylenediaminetetraacetic acid, 0.5 mM thiamine pyrophosphate, 1.5 mM Coenzyme A, 4 mM β-NAD^+, 1 mM DTT, 2 mM calcium chloride, and initiated with 15 mM 2-OG. Pyruvate carboxylase (PCX) activity was measured through the production of TNB^{2+} at a wavelength of 412 nm. The reaction mix contained 50 mM Tris HCl (pH 8), 50 mM sodium bicarbonate, 5 mM $MgCl_2$, 5 mM sodium pyruvate, 5 mM ATP, 0.5mM 5,5'-dithiobis-(2-nitrobenzoic acid), and 5 U/mL citrate synthase (C3260, Sigma Aldrich) and the reaction initiated with 0.1 mM acetyl CoA.

Mitochondrial coupling assay

Using the extracellular flux XFe96 Analyzer (Seahorse Bioscience, MA, USA), the degree of coupling between the electron transport chain, the oxidative phosphorylation machinery and ATP production was evaluated as previously described (Carrasco-Pozo et al., 2015; Tan et al., 2016).The contribution of the non-mitochondrial respiration to OCR was subtracted from

every mitochondrial function parameter. Respiration linked to ATP synthesis was calculated as state 3 ADP minus state 4o. All mitochondrial function parameters were normalized to protein content measured using a Pierce BCA Protein Assay Kit.

Mitochondrial electron flow.

The sequential electron flow through the complexes of the electron transport chain was studied using the extracellular flux XFe96 Analyzer as previously described (Carrasco-Pozo et al., 2015). This assay allows the study of the contribution and function of complexes I and II in the electron transport chain in terms of OCR. From the results, the complex I- (state 3u minus OCR after rotenone injection) and complex II-driven respiration (OCR after succinate injection minus OCR after malonate injection) were calculated.

Data Analysis

All statistical analyses were performed using GraphPad Prism version 6.0 (GraphPad Software, La Jolla, CA, USA). Two way ANOVAs, followed by uncorrected Fisher's Least Significant Differences post-tests were used for the total metabolite concentrations and percent enrichment comparisons. Correlation analysis was performed to assess the correlation of % ^{13}C enrichment of glucose 6-phosphate to downstream glycolytic intermediates and the % enrichment of pyruvate relative to TCA cycle intermediates enrichment. Enzyme activities and functional mitochondrial parameters were analysed using unpaired, two-sided student's t-tests. $P<0.05$ was regarded as significant. All data are represented as mean ± S.E.M.

Results

To assess the effects of pilocarpine-induced SE on brain glucose metabolism in mice in the chronic stage of the model, the total concentrations of glycolytic and TCA cycle

intermediates were measured using LC-MS/MS, along with the percent incorporation of ^{13}C from injected [U-^{13}C]-glucose (i.p.). Furthermore, mitochondrial electron transport functions were analysed, and the activities of enzymes involved in all pathways were measured using spectrophotometric assays.

Of the 25 mice that were injected with pilocarpine, 12 (48%) mice developed SE, classified as continuous whole-body clonic seizures. Eleven (44%) mice did not develop these seizures and thus were classified as "No SE", and two (8%) mice died from a seizure during the 90-minute observation period. From the twelve mice that developed SE, 2 mice were sacrificed in the following three days as per ethical guidelines, as they did not recover well from SE.

In this study, we injected mice 3 weeks after SE in the chronic stage of the model with [U-^{13}C]-glucose to obtain information of glucose metabolism in the glycolytic and TCA cycle pathways. At this time point the body weights of SE mice used for the [U-^{13}C]-glucose analysis were similar to the No SE group (39.9 ± 1.3g vs. 39.8 ± 0.8g, p=0.97). Therefore, any changes in the total concentrations or percent of ^{13}C enrichment in brain metabolites are not due to differing amounts of [U-^{13}C]-glucose injected. No behavioural seizures were observed before and during the [U-^{13}C]-glucose injection until sacrifice. The total concentrations of metabolites in the glycolytic pathway and TCA cycle were similar among mice that had developed SE compared to those that did not, as shown in Table 2.

Percent enrichment of ^{13}C in hippocampal glycolytic intermediates

As shown in Figure 2A, the chronic stage after SE has an effect on the percent enrichment of ^{13}C in the chronic stage of the pilocarpine model (Two-way ANOVA, $p<0.001$). Specifically, reductions were found in the ^{13}C enrichment of glucose 6-phosphate (22%), fructose 6-phosphate (21% reduction), dihydroxyacetone phosphate (17%) and phosphoenolpyruvate (20%) in the SE mice compared to those that did not develop SE (n=10-11, $p<0.05$-0.01 for

each metabolite in Fisher's LSD post test). No other significant differences were found in the percent enrichment in other glycolytic intermediates, including fructose 1,6- bisphosphate, pyruvate and the combined metabolites of 2- and 3-phosphoglycerate ($p>0.05$, $n=10$-11). The percent ^{13}C enrichment in all glycolytic intermediates are highly correlated to the % enrichment of the first metabolite of the pathway, glucose 6-phosphate in No SE mice ($r=0.76$-97, $p<0.05$-0.001, Figure 2C). In contrast no correlation was observed between the body weight of mice and the incorporation of ^{13}C in glucose 6-phosphate ($r=-0.28$, $p>0.05$). Figure 2C shows that this correlation was also observed in SE mice for all metabolites ($r=0.64$-0.91, $p<0.05$-0.001) apart from 2 and 3-phosphoglycerate ($r=0.10$, $p=0.78$). Similarly, no correlation was observed between body weight and % ^{13}C enrichment in glucose 6-phosphate ($r=-0.21$, $p>0.05$). This suggests that after the conversion of glucose to glucose 6-phosphate there is no alteration in the activity of the glycolytic pathway itself, but rather that glucose uptake is diminished in SE mice. No significant differences were observed between the body weight of either No SE or SE mice and the ^{13}C % enrichment of G6P (Figure 2C, No SE, $r=-0.28$, $p>0.05$; Figure 2D, SE, $r=-0.21$, $p>0.05$).

The maximal activities of all cytosolic enzymes involved in the glycolytic pathway, namely phosphoglucose isomerase, phosphofructokinase, pyruvate kinase were unaltered between No SE and SE mice in the chronic epileptic stage (Figure 2B), which is consistent with the interpretation of results from the ^{13}C analysis. No changes were found between the two groups regarding the activities of the other cytosolic enzymes lactate dehydrogenase, and glucose 6-phosphate dehydrogenase, responsible for the conversion of pyruvate to lactate and entry into the pentose phosphate pathway, respectively. It should be noted here that these enzymes, except glucose 6-phosphate dehydrogenase and phosphofructokinase, are not rate limiting.

% enrichment of ^{13}C in TCA cycle intermediates in the hippocampus

The percentage enrichment of ^{13}C in TCA cycle intermediates derived from [U-^{13}C]-glucose entering via pyruvate dehydrogenation were determined. We found a reduction in the % ^{13}C enrichment in the TCA cycle intermediates citrate (17%), aconitate (17%), succinate (34%), fumarate (24%) and malate (17%) in SE mice compared to No SE mice (all $p<0.05$-0.01, Figure 3A). 2-oxoglutarate was the only metabolite where no significant change in ^{13}C enrichment was observed between SE and No SE groups ($p=0.22$).

The ^{13}C labelled oxaloacetate produced when [1,2-^{13}C]-acetyl-CoA enters the TCA cycle for the first time can be traced through the second cycle of the TCA cycle, if it condenses with ^{13}C-labelled acetyl-CoA (Figure 3B). Decreases in the percentage enrichment of ^{13}C in the second turn of the TCA cycle were observed for 2-oxoglutarate (47%), succinate (54%), fumarate (25%) and malate (29%) in chronic SE mice (all $p<0.05$-0.01). No change in ^{13}C % enrichment was found in citrate ($p>0.05$).

Correlations were observed between the ^{13}C enrichments in pyruvate and those in first turn TCA cycle metabolites resulting from pyruvate metabolism via PDH in No SE mice ($r=0.70$-0.31, $p<0.01$-0.001; Figure 3D). This correlation was lost in SE mice ($r=0.34$-0.54, $p>0.1$-0.3), suggesting that there is another factor that determines entry of pyruvate into the TCA cycle in the chronic epileptic stage (Figure 3E).

The maximal activity of the mitochondrial enzyme PDH, responsible for the entry of pyruvate into the TCA cycle was reduced by 33% in chronic SE mice compared to No SE mice (Figure 3C, $p<0.05$). The maximal specific activity of OGDH, the rate-limiting enzyme of TCA cycling was reduced by 55% in the SE mice ($p<0.05$). Similar activities were observed in the other mitochondrial enzymes pyruvate carboxylase, glutamate dehydrogenase, glutamic pyruvic transaminase and glutamic oxaloacetic transaminase ($p>$

0.05 for all enzymes), suggesting that the changes in PDH and OGDH activities were not due to loss of mitochondria. A strong correlation of the % enrichments within 2-oxoglutarate to those of succinate is observed in individual No SE mice (Figure 3F, $r=0.95$, $p<0.001$), indicating that ^{13}C enrichments of these two metabolites are highly dependent on each other. This correlation is lost in the SE mice, indicating that another factor such as the found altered OGDH activity plays a role ($r=0.29$, $p=0.42$).

Mitochondrial coupling assays using the extracellular flux

Various functional parameters of the mitochondria isolated from the hippocampal formation were measured using the extracellular XF96 Analyzer. Similar results were observed in all functional parameters regarding the coupling assay (Figure 4A) and the electron transport chain (Figure 4B). This includes state 2, state 3 ADP, state 3u and oxygen consumption linked to ATP synthesis (Figure 4C-F). In addition, similar results were found in the complex I- and complex II-driven respirations of No SE and SE mice (Figure 4G, H). Thus, there is no indication of general, mitochondrial dysfunction in the chronic "epileptic" brain in this mouse model.

Discussion

Here we show direct evidence that glucose metabolism is lower in a chronic epilepsy mouse model due to the decrease in the ^{13}C incorporation into intermediates of both glycolysis (Figure 2A) and the TCA cycle (Figure 3A and B). Moreover, there was loss of activity in two rate limiting enzymes of the TCA cycle, PDH and OGDH. No changes were found in the maximal activity of any enzymes involved in glycolysis. Lastly, similar rates of oxygen consumption were measured in hippocampal mitochondria from No SE and SE mice, indicating that the electron transport chain and ATP synthase are not affected in this model.

Please note, we have previously shown using video–electroencephalography recordings that during the chronic phase of this model mice experience 1-2 spontaneous seizures a day (Benson et al., 2015). Mice were not experiencing behavioural seizures before and while sacrificed, thus these findings reflect changes in interictal glucose metabolism.

Following the injection of [U-^{13}C]-glucose, the incorporation of ^{13}C into several glycolytic intermediates was reduced in the hippocampal formation, including glucose 6-phosphate, fructose 6-phosphate, dihydroxyacetone phosphate and phosphoenolpyruvate. To our knowledge no previous study has investigated the changes in glucose metabolism in chronic epilepsy via the quantification of glycolytic intermediates. Earlier studies have assessed lactate or alanine concentrations as indicators for changes in glycolysis with mixed results. In our earlier study in the same mouse model, there was no change in the ^{13}C enrichment in either lactate or alanine after injection of [1,2-^{13}C]-glucose (Smeland et al., 2013). Similarly, no alterations in the amounts of these intermediates were observed 24 hours after kainate induced SE in rats (Qu et al., 2003). However, reduced [3-^{13}C]-alanine from [1-^{13}C]-glucose metabolism was observed in the chronic lithium pilocarpine rat SE model, without a change in [3-^{13}C]-lactate concentrations (Melo et al., 2005). This was interpreted as defects in mitochondrial metabolism as alanine can be metabolized in both mitochondria and the cytosol, whereas lactate is purely produced in the cytosol. Both lactate and alanine are products of pyruvate metabolism in the cytosol, while pyruvate also enters the mitochondria to produce products of the TCA cycle via PDH, pyruvate carboxylase or glutamic pyruvic transaminase. Therefore, a change in the concentrations of either alanine or lactate can be reflective of an alteration of glycolytic or the TCA cycle activity that leads to an imbalance of the activities of these two pathways (Greene et al., 2003). Our current data of lowered enrichment of ^{13}C in glycolytic intermediates in SE mice together with our earlier result of unchanged [3-^{13}C]-lactate and [3-^{13}C]-alanine concentrations indicate that less [U-^{13}C]-

pyruvate must be metabolized to acetyl-CoA to maintain similar incorporation of the label into lactate and alanine compared to No SE mice. This is also corroborated by our finding of decreased PDH activity.

A limitation of this study was the inability to measure both the total concentration and the enrichment of ^{13}C in glucose. Thus, we do not have any direct indications for potential alterations of glucose uptake by the epileptic brain, although previous studies showed reduced glucose uptake in adult rats in the chronic stage (see below). Because no changes were found in the activities of any regulatory enzymes in the glycolytic pathway, including hexokinase, phosphofructokinase and pyruvate kinase, it is unlikely that glycolytic activity itself is impaired. Moreover, correlation analysis (Figure 2C and D) of the ^{13}C enrichment shows that in both No SE and SE mice there was a strong correlation between the enrichment of ^{13}C in glucose 6-phosphate and most downstream metabolites. Furthermore, a lack of correlation was evident between the body weight of mice, which determined the amount of [U-^{13}C]-glucose injected and the ^{13}C enrichment of glucose 6-phosphate. Together this suggests that chronic epilepsy does not alter glycolysis, and thus the lower incorporation of ^{13}C in SE mice is due to reduced uptake of glucose in the hippocampus, but not the activity of this pathway itself. This indicates that if glucose uptake was restored in this chronic epileptic state no impairment would be observed in the glycolytic pathway.

Several studies using ^{18}FDG-PET have shown that interictal glucose uptake in patients is reduced (Henry et al., 1990; Henry et al., 1993; Arnold et al., 1996). Similarly, in the rodent lithium-pilocarpine model of epilepsy, glucose uptake is also reduced during the chronic phase (Dubé et al., 2001; Lee et al., 2012). Both these studies also provided evidence of neuronal loss in regions of reduced glucose uptake, which may at least in part be responsible for reduced glucose uptake. Previously hippocampal neuronal loss has been characterized in

the mouse pilocarpine model (Borges et al., 2003a) and may also contribute to the results of our study. However, several studies have failed to correlate neuronal loss with glucose metabolism (O'Brien et al., 1997; Dubé et al., 2001), suggesting that changes in interictal glucose metabolism are not wholly due to neuronal loss. Our study now provides the first evidence that although glucose uptake is reduced within the hippocampus of the chronic epileptic brain and less glucose overall seems to be metabolized, the glycolytic pathway itself is unimpaired.

The other key finding of this study is a reduction of the ^{13}C enrichment in the TCA cycle intermediates following entry of [1,2-^{13}C]-acetyl CoA via PDH (Figure 3A, B), as well as in the second turn of the TCA cycle. This can be partially explained by the reduced ^{13}C enrichment in the glycolytic intermediates, and thus there is less [1,2-^{13}C]-acetyl CoA available to form citrate. However, in No SE mice the ^{13}C enrichment of pyruvate is highly correlated to the ^{13}C enrichment in TCA cycle metabolites from the first turn in the TCA cycle (Figure 3D). This correlation is lost in the SE mice, which suggests that in the chronically epileptic mice there are other factors that influence entry of pyruvate into the TCA cycle (Figure 3E), such as the 33% reduction found in PDH activity (Figure 3C). Consistent with this, patients with mutations in the PDH complex that lead to deficient activity are known to present with epileptic phenotypes (Kang et al., 2007; Barnerias et al., 2010).

In this study, we also observed a loss of 55% of the maximal activity of 2-oxoglutarate dehydrogenase, the rate limiting enzyme of TCA cycling (Figure 3C). This enzyme shares the E3 subunit, dihydrolipoamide dehydrogenase with the pyruvate dehydrogenase complex. This subunit is a flavin-containing protein, which reduces NAD^+ to NADH through the

433 transfer of reducing equivalents from the dihydrolyl moiety (Carothers et al., 1989).
434 Heterozygous knockout of this protein in mice has shown to reduce activity of both PDH and
435 OGDH complexes, and the mice are more prone to neurodegenerative disorders (Gibson et
436 al., 2000). In autopsied patients with Alzheimer's disease the protein concentrations of all
437 subunits of OGDH were reduced compared to control patients in the cortex, with the loss of
438 the E3 subunit protein being restricted to the hippocampus (Mastrogiacomo et al., 1996).
439 Reduced activity was found in several other neurological disorders as previously summarized
440 (Kish, 1997). In a separate study the activities of both OGDH and PDH were reduced in
441 autopsied Alzheimer's disease patients and were correlated to the severity of the disease
442 (Bubber et al., 2005). Although the mechanisms behind reduced PDH and OGDH activity
443 are currently unknown, they may be potential new targets to increase energy metabolism in
444 chronic epilepsy and neurodegenerative disorders.
445
446 The change in PDH and OGDH activities also supports the further reduction found in the ^{13}C
447 enrichment in metabolites that entered the second turn of the TCA cycle produced when ^{13}C
448 oxaloacetate condenses with [1,2-^{13}C]-acetate (Figure 3B). Together these results
449 demonstrate that TCA cycling is impaired in the hippocampus in the chronic stage of the
450 pilocarpine model, which agrees with previous studies in both rat and mice chronic SE
451 models that show reduced incorporation of ^{13}C from glucose metabolism into the amino acids
452 glutamate, GABA and aspartate (Qu et al., 2003; Melo et al., 2005; Smeland et al., 2013).
453
454 We found similar mitochondrial oxygen consumption rates related to proton leak, ATP
455 synthesis, coupling efficiency and respiratory control ratio (Figure 4C-F), which indicates
456 lack of mitochondrial dysfunction in the electron transport chain and its involvement in the
457 final steps of oxidative phosphorylation in this chronic model of epilepsy. Mitochondrial

458 dysfunction has been found acutely following both kainate- and pilocarpine- induced seizures
459 (Chuang et al., 2004; Carrasco-Pozo et al., 2015). However, we have previously shown that
460 this dysfunction is transient as no changes were found in any functional parameters 48 hours
461 after SE (Carrasco-Pozo et al., 2015), which is further supported by our results during the
462 chronic phase.
463
464 It is difficult to assess to which extent the impairments in TCA cycle activity found here are
465 the result of chronic recurrent seizures. However, together with reduction in glucose uptake
466 and reduced TCA cycling will result in less ATP production in the hippocampus. This is
467 highly likely to contribute to the generation of seizures as well as seizure spread within the
468 brain, as ATP is critical for most cellular functions and the maintenance of membrane
469 potentials, and a loss of ATP can lead to hyperexcitability. This is evidenced by the
470 proconvulsant effects of toxins blocking the respiratory chain and ATP production, such as
471 3-nitropropionic acid (Haberek et al., 2000)as well as by the many patients with epileptic
472 seizures due to inherited TCA and respiratory chain enzyme deficiencies (Burgeois et al.,
473 1992; Barnerias et al., 2010; Khurana et al., 2013).
474
475 **Conclusions**
476 In the chronic epileptic stage, glycolytic enzymatic activities and the metabolism of glucose
477 6-phosphate were unimpaired in the hippocampal formation. However, glucose uptake is
478 likely to be reduced in mice in the chronic "epileptic" stage, which reduced the incorporation
479 of ^{13}C from injected [U-^{13}C]-glucose (i.p.) into glycolytic intermediates. Also, there was
480 decreased pyruvate entry into the TCA cycle via PDH and reduced TCA cycling, including
481 decreased activity of OGDH, in this chronic epilepsy model. Together, this will lead to
482 reduced ATP production despite unaltered activity of the electron transport chain and ATP

synthase in the hippocampus, which is likely to contribute to seizures. In summary, these data revealed several potential metabolic targets to inhibit seizure generation in an epileptic brain.

References

Alvestad S, Hammer J, Qu H, Håberg A, Ottersen OP, Sonnewald U (2011) Reduced astrocytic contribution to the turnover of glutamate, glutamine, and GABA characterizes the latent phase in the kainate model of temporal lobe epilepsy. Journal of Cerebral Blood Flow & Metabolism 31:1675-1686.

Arnold S, Schlaug G, Niemann H, Ebner A, Luders H, Witte O, Seitz R (1996) Topography of interictal glucose hypometabolism in unilateral mesiotemporal epilepsy. Neurology 46:1422-1422.

Avoli M, De Curtis M, Gnatkovsky V, Gotman J, Köhling R, Lévesque M, Manseau F, Shiri Z, Williams S (2016) Specific imbalance of excitatory/inhibitory signaling establishes seizure onset pattern in temporal lobe epilepsy. Journal of neurophysiology:jn. 01128.02015.

Barnerias C, Saudubray JM, Touati G, De Lonlay P, Dulac O, Ponsot G, Marsac C, Brivet M, Desguerre I (2010) Pyruvate dehydrogenase complex deficiency: four neurological phenotypes with differing pathogenesis. Dev Med Child Neurol 52:e1-9.

Benson MJ, Manzanero S, Borges K (2015) Complex alterations in microglial M1/M2 markers during the development of epilepsy in two mouse models. Epilepsia 56:895-905.

Borges K, Gearing M, McDermott DL, Smith AB, Almonte AG, Wainer BH, Dingledine R (2003a) Neuronal and glial pathological changes during epileptogenesis in the mouse pilocarpine model. Experimental Neurology 182:21-34.

508 Borges K, Gearing M, McDermott DL, Smith AB, Almonte AG, Wainer BH, Dingledine R
509 (2003b) Neuronal and glial pathological changes during epileptogenesis in the mouse
510 pilocarpine model. Experimental neurology 182:21-34.
511 Bubber P, Haroutunian V, Fisch G, Blass JP, Gibson GE (2005) Mitochondrial abnormalities
512 in Alzheimer brain: mechanistic implications. Annals of neurology 57:695-703.
513 Burgeois M, Goutieres F, Chretien D, Rustin P, Munnich A, Aicardi J (1992) Deficiency in
514 complex II of the respiratory chain, presenting as a leukodystrophy in two sisters with
515 Leigh syndrome. Brain Dev 14:404-408.
516 Carothers DJ, Pons G, Patel MS (1989) Dihydrolipoamide dehydrogenase: functional
517 similarities and divergent evolution of the pyridine nucleotide-disulfide
518 oxidoreductases. Archives of biochemistry and biophysics 268:409-425.
519 Carrasco-Pozo C, Tan KN, Borges K (2015) Sulforaphane is anticonvulsant and improves
520 mitochondrial function. Journal of Neurochemistry 135:932-942.
521 Chuang YC, Chang AY, Lin JW, Hsu SP, Chan SH (2004) Mitochondrial Dysfunction and
522 Ultrastructural Damage in the Hippocampus during Kainic Acid–induced Status
523 Epilepticus in the Rat. Epilepsia 45:1202-1209.
524 Chugani HT, Chugani DC (1999) Basic mechanisms of childhood epilepsies: studies with
525 positron emission tomography. Advances in neurology 79:883.
526 Dube C, Boyet S, Marescaux C, Nehlig A (2001) Relationship between neuronal loss and
527 interictal glucose metabolism during the chronic phase of the lithium-pilocarpine
528 model of epilepsy in the immature and adult rat. Experimental neurology 167:227-
529 241.
530 Dubé C, Boyet S, Marescaux C, Nehlig A (2001) Relationship between neuronal loss and
531 interictal glucose metabolism during the chronic phase of the lithium-pilocarpine

model of epilepsy in the immature and adult rat. Experimental neurology 167:227-241.

Escayg A, Goldin AL (2010) Sodium channel SCN1A and epilepsy: mutations and mechanisms. Epilepsia 51:1650-1658.

Gibson GE, Park LC, Sheu K-FR, Blass JP, Calingasan NY (2000) The α-ketoglutarate dehydrogenase complex in neurodegeneration. Neurochemistry international 36:97-112.

Greene AE, Todorova MT, Seyfried TN (2003) Perspectives on the metabolic management of epilepsy through dietary reduction of glucose and elevation of ketone bodies. J Neurochem 86:529-537.

Haberek G, Tomczyk T, Zuchora B, Wielosz M, Turski WA, Urbanska EM (2000) Proconvulsive effects of the mitochondrial respiratory chain inhibitor — 3-nitropropionic acid. European Journal of Pharmacology 403:229-233.

Hadera MG, Smeland OB, McDonald TS, Tan KN, Sonnewald U, Borges K (2013) Triheptanoin partially restores levels of tricarboxylic acid cycle intermediates in the mouse pilocarpine model of epilepsy. Journal of Neurochemistry.

Henry TR, Mazziotta JC, Engel J (1993) Interictal metabolic anatomy of mesial temporal lobe epilepsy. Archives of Neurology 50:582-589.

Henry TR, Mazziotta JC, Engel J, Christenson PD, Zhang JX, Phelps ME, Kuhl DE (1990) Quantifying interictal metabolic activity in human temporal lobe epilepsy. Journal of Cerebral Blood Flow & Metabolism 10:748-757.

Kang HC, Kwon JW, Lee YM, Kim HD, Lee HJ, Hahn SH (2007) Nonspecific mitochondrial disease with epilepsy in children: diagnostic approaches and epileptic phenotypes. Childs Nerv Syst 23:1301-1307.

556 Ke C-J, He Y-H, He H-W, Yang X, Li R, Yuan J (2014) A new spectrophotometric assay for
557 measuring pyruvate dehydrogenase complex activity: a comparative evaluation.
558 Analytical Methods 6:6381-6388.
559 Khurana DS, Valencia I, Goldenthal MJ, Legido A (2013) Mitochondrial Dysfunction in
560 Epilepsy. Seminars in Pediatric Neurology 20:176-187.
561 Kish SJ (1997) Brain Energy Metabolizing Enzymes in Alzheimer's Disease: α-Ketoglutarate
562 Dehydrogenase Complex and Cytochrome Oxidasea. Annals of the New York
563 Academy of Sciences 826:218-228.
564 Kuhl DE, Engel J, Phelps ME, Selin C (1980) Epileptic patterns of local cerebral metabolism
565 and perfusion in humans determined by emission computed tomography of 18FDG
566 and 13NH3. Annals of Neurology 8:348-360.
567 Le Belle J, Harris N, Williams S, Bhakoo K (2002) A comparison of cell and tissue
568 extraction techniques using high-resolution 1H-NMR spectroscopy. NMR in
569 Biomedicine 15:37-44.
570 Lee EM, Park GY, Im KC, Kim ST, Woo CW, Chung JH, Kim KS, Kim JS, Shon YM, Kim
571 YI (2012) Changes in glucose metabolism and metabolites during the epileptogenic
572 process in the lithium-pilocarpine model of epilepsy. Epilepsia 53:860-869.
573 Mastrogiacomo F, Lindsay JG, Bettendorff L, Rice J, Kish SJ (1996) Brain protein and α-
574 ketoglutarate dehydrogenase complex activity in alzheimer-s disease. Annals of
575 neurology 39:592-598.
576 McDonald TS, Tan KN, Hodson MP, Borges K (2013) Alterations of hippocampal glucose
577 metabolism by even versus uneven medium chain triglycerides. Journal of Cerebral
578 Blood Flow & Metabolism.
579 Medina-Torres CE, van Eps AW, Nielsen LK, Hodson MP (2015) A liquid chromatography–
580 tandem mass spectrometry-based investigation of the lamellar interstitial metabolome

in healthy horses and during experimental laminitis induction. The Veterinary Journal 206:161-169.

Melo TM, Nehlig A, Sonnewald U (2005) Metabolism is normal in astrocytes in chronically epileptic rats: a (13)C NMR study of neuronal-glial interactions in a model of temporal lobe epilepsy. Journal of cerebral blood flow and metabolism : official journal of the International Society of Cerebral Blood Flow and Metabolism 25:1254-1264.

Mulley JC, Scheffer IE, Petrou S, Dibbens LM, Berkovic SF, Harkin LA (2005) SCN1A mutations and epilepsy. Human mutation 25:535-542.

O'Brien TJ, Newton MR, Cook MJ, Berlangieri SU, Kilpatrick C, Morris K, Berkovic SF (1997) Hippocampal Atrophy Is Not a Major Determinant of Regional Hypometabolism in Temporal Lobe Epilepsy. Epilepsia 38:74-80.

Qu H, Eloqayli H, Müller B, Aasly J, Sonnewald U (2003) Glial–neuronal interactions following kainate injection in rats. Neurochemistry international 42:101-106.

Smeland OB, Hadera MG, McDonald TS, Sonnewald U, Borges K (2013) Brain mitochondrial metabolic dysfunction and glutamate level reduction in the pilocarpine model of temporal lobe epilepsy in mice. Journal of Cerebral Blood Flow & Metabolism.

Tan KN, McDonald TS, Borges K (2015) Metabolic dysfunctions in epilepsy and novel metabolic treatment approaches.

Tan KN, Carrasco-Pozo C, McDonald TS, Puchowicz M, Borges K (2016) Tridecanoin is anticonvulsant, antioxidant, and improves mitochondrial function. Journal of Cerebral Blood Flow & Metabolism.

Vezzani A, French J, Bartfai T, Baram TZ (2011) The role of inflammation in epilepsy. Nature Reviews Neurology 7:31-40.

606 Vielhaber S, Von Oertzen JH, Kudin AF, Schoenfeld A, Menzel C, Biersack HJ, Kral T,
607 Elger CE, Kunz WS (2003) Correlation of Hippocampal Glucose Oxidation Capacity
608 and Interictal FDG-PET in Temporal Lobe Epilepsy. Epilepsia 44:193-199.

609
610
611
612
613
614
615
616
617
618
619
620
621
622
623
624
625
626
627
628
629

Figure 1: Schematic of [U-^{13}C]-glucose in the brain. Simplified schematic of ^{13}C-labelling patterns following the metabolism of [U-^{13}C]-glucose via glycolysis and the TCA cycle. Empty circles represent ^{12}C and black filled circle represent ^{13}C. The grey filled circles represent ^{13}C derived from ^{13}C-labelled oxaloacetate that enters the 2nd turn of the TCA cycle (grey dotted lines). * Stars indicate the metabolites that were not measured in this study. Glucose 6-phosphate (G6P); fructose 6-phosphate (F6P); fructose 1,6-bisphosphate (F16BP); glyceraldehyde 3-phosphate (GA3P); dihydroxyacetone phosphate (DHAP); 1,3-bisphosphoglycerate (13BPG); 3-phosphoglycerate (3PG); 2-phosphoglycerate (2PG); phosphoenolpyruvate (PEP); pyruvate (PYR); Acetyl CoA (Ac-CoA); citrate (CIT); aconitate (ACO); 2-oxoglutarate (2OG); succinate (SUC); fumarate (FUM); malate (MAL); oxaloacetate (OAA).

Figure 2: Metabolism of [U-^{13}C]-glucose via glycolysis in SE mice in the chronic stage of pilocarpine model. A) Hippocampal ^{13}C enrichment of glycolytic metabolites after i.p. injection of [U-^{13}C]-glucose was compared between SE and No SE mice. Reduced ^{13}C enrichment in SE mice was found in glucose 6-phosphate (G6P, 22% reduction, $p=0.030$), fructose 6-phosphate (F6P, 21%, $p=0.038$), dihydroxyacetone phosphate (DHAP, 17%, $p=0.05$) and phosphoenolpyruvate (PEP, 20%, $p=0.023$). No significant differences were found in fructose 1,6-bisphosphate (F16BP), 2 and 3 phosphoglycerate (2+3PG), and pyruvate (PYR). Two-way ANOVA, SE status $p<0.001$, n=9-11 mice. **B)** The activities of all cytosolic enzymes, namely hexokinase (HK), phosphoglucose isomerase (PGI), phosphofructokinase (PFK), pyruvate kinase (PK), lactate dehydrogenase (LDH), and glucose 6-phosphate dehydrogenase (G6PDH) were unaltered between control No SE mice and mice after SE within the chronic stage of the model ($p>0.05$ for all). n=7-9. **C)** Correlation analysis between the % ^{13}C enrichment of G6P and the ^{13}C enrichment in

downstream metabolites in No SE mice. A significant correlation was observed with each metabolite specifically F6P, r=0.89, p<0.001; F16BP, r=0.97, p<0.001; DHAP r=0.96, p<0.001; 2+3PG r=0.76, p<0.01; PEP, r=0.96, p<0.001; PYR, r=0.95, p<0.001). No significant correlation was found between body weight (g) and % ^{13}C enrichment of G6P, r=-0.28, p>0.05. **D)** Correlation analysis between the % ^{13}C enrichment of G6P and the ^{13}C enrichment in downstream metabolites in SE mice. Similar to the No SE group a strong correlation was observed with each downstream metabolite apart from 2+3PG. F6P, r=0.91, p<0.001; F16BP, r=086, p<0.001; DHAP, r=0.90, p<0.001; 2+3PG, r=0.10, p>0.05; PEP, r=0.72, p<0.05, PYR, r=0.64, p<0.05). No significant correlation was found between body weight (g) and % ^{13}C enrichment of G6P, r=-0.21, p>0.05.

Figure 3: Metabolism of [U-^{13}C]-glucose via the TCA cycle is impaired in SE mice in the chronic stage of pilocarpine model. A) Percent ^{13}C enrichment in the TCA cycle metabolites from the first turn of the TCA cycle were compared between SE and No SE mice. Reduced ^{13}C enrichment was found in citrate (CIT, 17% reduction, p<0.006), aconitate (ACO, 17%, p=0.0001), succinate (SUC, 35%, p=0.005), and fumarate (FUM, 23%, p=0.001) in the hippocampal formation of mice in the chronic epileptic state. No changes were found in the ^{13}C enrichment of 2-oxoglutarate (2OG, p>0.05) or malate (MAL, p>0.05). Two-way ANOVA, SE status p<0.001, n=9-11 mice. **B)** The percent ^{13}C enrichment of TCA cycle metabolites when labelled oxaloacetate condenses with [1,2-13C]-acetyl CoA. A reduction in ^{13}C enrichment was observed in the intermediates 2OG (47%, p=0.03), SUC (55%, p=0.037), FUM (25%, p=0.044) and MAL (29%, p=0.003). Two-way ANOVA, Seizure status p<0.001. n=9-11 mice. **C)** Maximal activities of mitochondrial enzymes were compared between SE and No SE mice. SE mice had lower activity of both pyruvate dehydrogenase (PDH, 33%, p=0.045) and 2-oxoglutarate dehydrogenase (OGDH, 55%,

p=0.027) two key enzymes involved in the entry and rate of TCA cycling compared to No SE controls. No changes were found in the enzymes pyruvate carboxylase (PC), glutamate dehydrogenase (GDH), glutamic pyruvic transaminase (GPT), and glutamic oxaloacetic transaminase (GOT, all p>0.05). N=7-9 mice for all enzymes. **D)** Correlation analysis between the percent ^{13}C enrichment in pyruvate to all first turn TCA cycle intermediates in No SE mice. A significant correlation exists for all metabolites when compared to pyruvate in this group. CIT, r=0.86, p<0.001; ACO, r=0.80, p<0.01; 2OG, r=0.78, p<0.01; SUC, r=0.86, p<0.01; FUM, r=0.70, p=<0.05; MAL, r=0.91, p<0.001. **E)** Correlation analysis between ^{13}C enrichment (%) in SE mice between pyruvate and first turn TCA cycle intermediates. No significant correlation was found between pyruvate and the TCA cycle metabolites. CIT, r=0.34, p>0.05; ACO, r=0.54, p>0.05; 2OG, r=0.40, p>0.05; SUC, r=0.48, p>0.05; FUM, r=0.37, p>0.05; MAL, r=0.46, p>0.05. **F)** Correlation between the % enrichment of ^{13}C from the first turn of the TCA cycle between 2OG and SUC. A strong correlation was observed between the ^{13}C enrichment in the two metabolites in No SE mice (r=0.95, p<0.001), while no correlation was found in the ^{13}C enrichment of 2OG and SUC in SE mice (r=0.42, p>0.05).

Figure 4: Mitochondrial functional parameters of isolated hippocampal mitochondria from SE and no SE mice measured with the extracellular flux analyser. **A)** Representation of the stages of the coupling assay to measure mitochondrial functions based on oxygen consumption rate (OCR). **B)** An example of the stages of the electron flow assay to measure electron flow through the electron transport chain base on the OCR. No differences were found in any of the parameters measured using the coupling assay **C)** state 2 respiration, **D)** state 3 respiration following the addition of ADP, **E)** state 3 uncoupled respiration, and F) respiration associated with ATP synthesis. Similarly, no significant

differences were observed in the parameters measured using the electron flow assay including **G)** complex I driven respiration and **H)** complex II driven respiration between No SE and SE mic (n=6-8 mice).

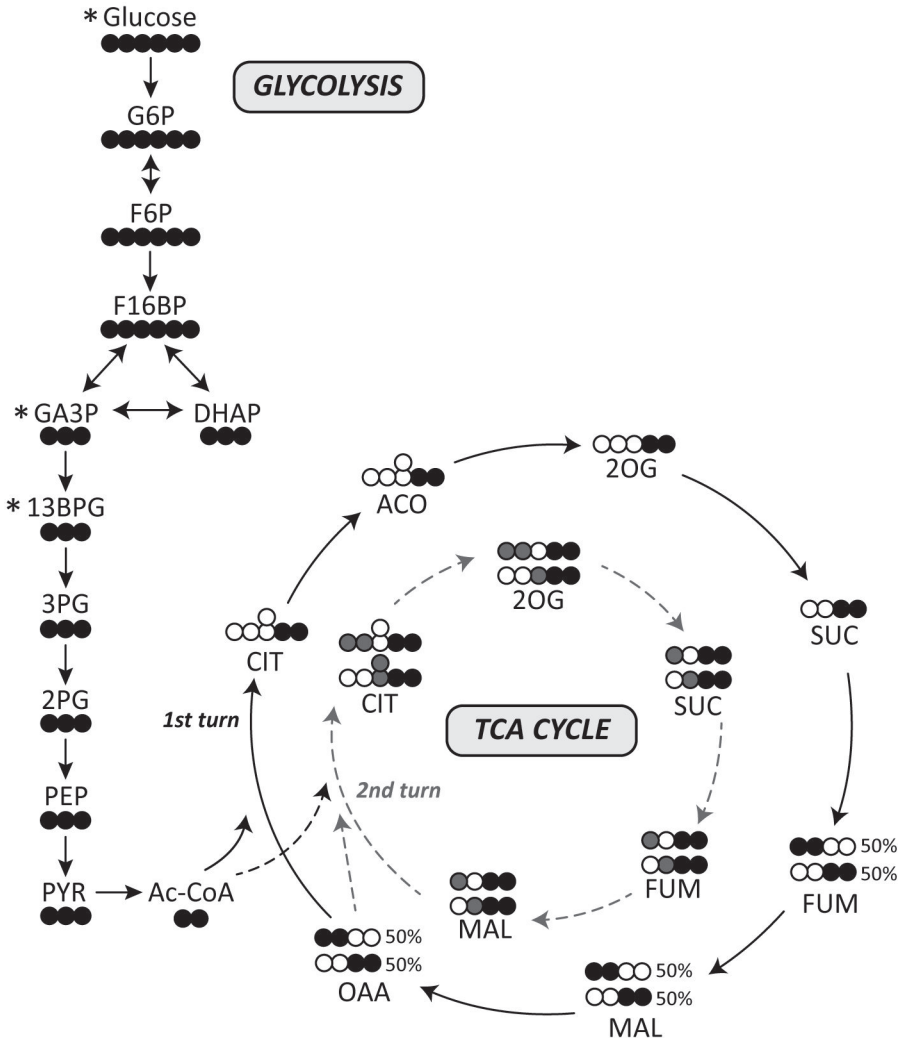

Figure 2

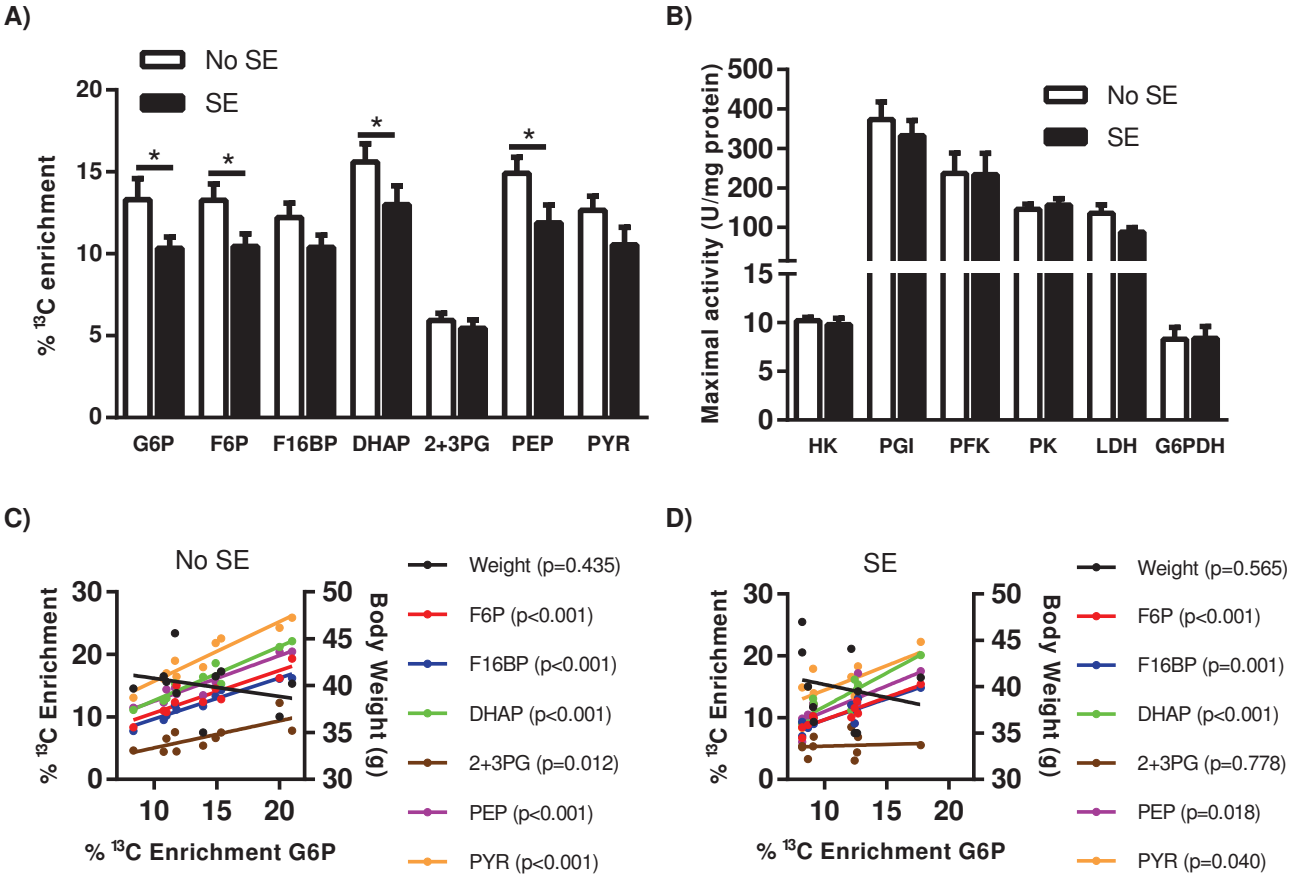

Figure 3

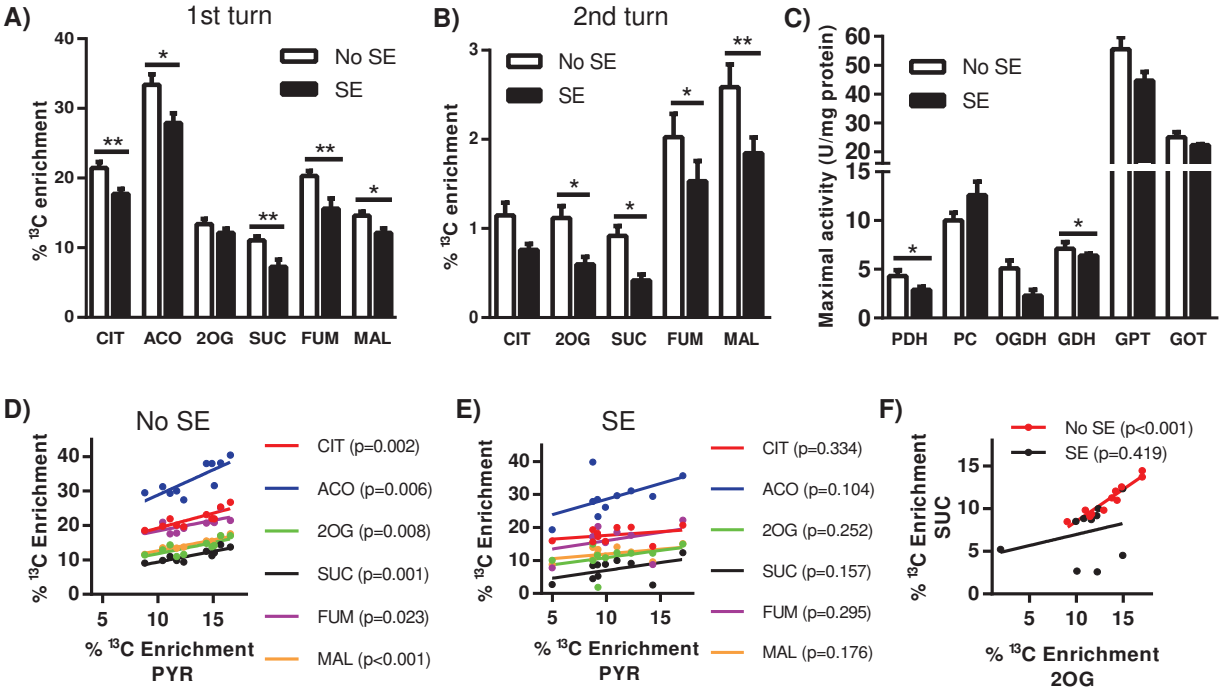

Figure 4

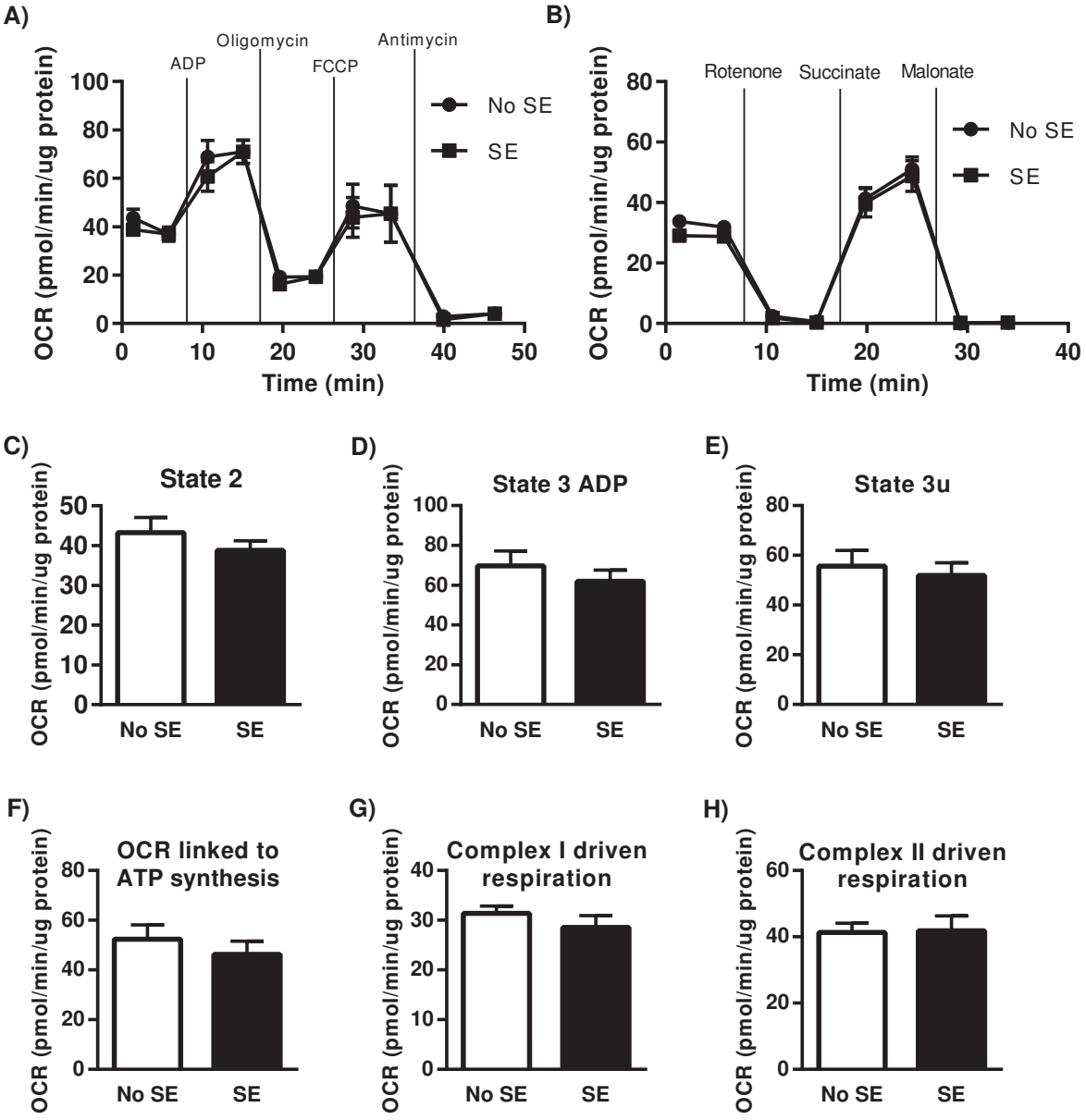

Table 1. Analyte-dependent parameters for the transitions used in scheduled multiple reaction monitoring data acquisition

Analyte	Q1 (Da) ^{12}C Analyte	Q3 (Da) ^{12}C Analyte	RT (min)	DP (volts)	CE (volts)	CXP (volts)
Glucose 6-phosphate	258.89	96.7	8.1	-20	-30	-15
Fructose 6-bisphosphate	259.02	96.8	9.6	-20	-30	-15
Fructose 1,6-bisphosphate	339.08	96.9	21.9	-20	-30	-15
Dihydroxyacetone phosphate	168.84	97	11.9	-50	-14	-5
2+3-phosphoglycerate	184.91	97	21.5	-50	-20	-5
Phosphoenolpyruvate	166.83	79	22.3	-40	-18	-5
Pyruvate	87.02	43	11.9	-45	-12	-1
Citrate	190.96	110.9	22.6	-50	-18	-7
Aconitate	172.94	84.9	22.6	-30	-18	-5
2-oxoglutarate	144.95	100.8	20.5	-40	-12	-5
Succinate	117	73	18.5	-45	-16	-3
Fumarate	115.01	70.9	21.1	-45	-12	-1
Malate	133	70.8	19.7	-40	-22	-3

Table 2. Total levels of metabolites

nmol/g tissue	No SE (n=6-9)	SE (n=6-7)
Glucose 6-phosphate	20.1 ± 1.7	24.2 ± 3.4
Fructose 6-phosphate	33.0 ± 2.2	36.2 ± 5.9
Fructose 1,6-bisphosphate	16.5 ± 1.0	17.8 ± 1.4
Dihydroxyacetone phosphate	0.70 ± 0.08	0.67 ± 0.08
2+3-phosphoglycerate	11.2 ± 1.0	10.9 ± 1.2
Phosphoenolpyruvate	8.93 ± 1.42	7.50 ± 1.33
Pyruvate	38.2 ± 2.7	34.2 ± 6.0
Citrate	109 ± 5	110 ± 17
Aconitate	1.84 ± 0.12	2.24 ± 0.28
2-oxoglutarate	90.8 ± 6.5	83.9 ± 17.4
Succinate	10.1 ± 0.8	8.1 ± 1.6
Fumarate	12.5 ± 0.9	13.2 ± 2.7
Malate	45.9 ± 3.9	46.1 ± 6.8